

## Methods and Applications

# A Prediction Model and Method for Indoor Radon Concentration by A Radon Simulation Chamber

Shuyuan Liu<sup>1</sup>; Li Zhang<sup>2</sup>; Wei Cheng<sup>3</sup>; Yongzhong Ma<sup>4</sup>; Kuke Ding<sup>1,2,#</sup>

## ABSTRACT

**Introduction:** This study aimed to establish a new predictive model for indoor radon concentrations.

**Methods:** We constructed a radon experimental model using prefabricated block walls and measured surface radon exhalation rates across multi-layer walls. The geometric parameters of various building envelopes (walls, floors, and roofs) were incorporated to calculate indoor radon concentrations from each source. Natural ventilation rates were also considered in developing the indoor radon concentration prediction model.

**Results:** Using closed-loop measurements, we determined the surface radon exhalation rates of prefabricated block walls and established fitting functions for multiple walls under varying temperatures and thicknesses. Based on indoor geometric parameters and natural ventilation rates, we developed a comprehensive prediction model for indoor radon concentrations. The model accurately predicted indoor equilibrium radon concentrations from prefabricated walls (thickness 0.155–0.268 m) at 23 °C, with deviations less than 10% from measured values within ventilation rates of 0.115±0.015 /h.

**Conclusions:** This scientifically rigorous and practical approach to predicting radon concentration, based on building composition and measurements of radon exhalation rates, enables proactive assessment of indoor radon concentrations and facilitates evidence-based health risk prevention strategies.

Radon (<sup>222</sup>Rn), a naturally occurring radioactive gas, is the second leading cause of lung cancer and has been associated with leukemia (1–4). The concentration of indoor radon has become an increasing public health concern. To protect public health, it is essential to incorporate predictive modeling of indoor radon levels during the architectural design phase. Such modeling enables optimal selection of

building locations, appropriate sizing of doors and windows, and evidence-based selection of construction materials. By optimizing building structural parameters, it becomes possible to prevent elevated indoor radon levels before construction completion, thereby safeguarding public health. Therefore, developing an accurate indoor radon concentration prediction model is crucial.

## METHODS

### Prefabrication of the Block Walls and Construction of A Radon Experimental Model

A device for measuring radon concentration is illustrated in Figure 1. The prefabricated block wall was sealed by applying an anti-radon coating to four or five surfaces, leaving one or two surfaces exposed for testing.

### Calculation of the Surface Radon Exhalation Rate from Various Source Items in Indoor Buildings

To determine indoor radon concentrations originating from building envelopes, we first established a fitting function for radon exhalation rate as a function of temperature and thickness using multivariate nonlinear regression analysis. We then calculated the total radon contribution by multiplying the surface area of each building envelope by its respective radon exhalation rate. For structures with curved interior surfaces, as illustrated in Figure 2, we employed geometric transformation relations to compute the effective surface area.

### Establishment of a Prediction Model for Indoor Radon Concentration Under Natural Air Exchange Conditions

We developed a prediction model for indoor radon concentration that accounts for radon exhalation rate

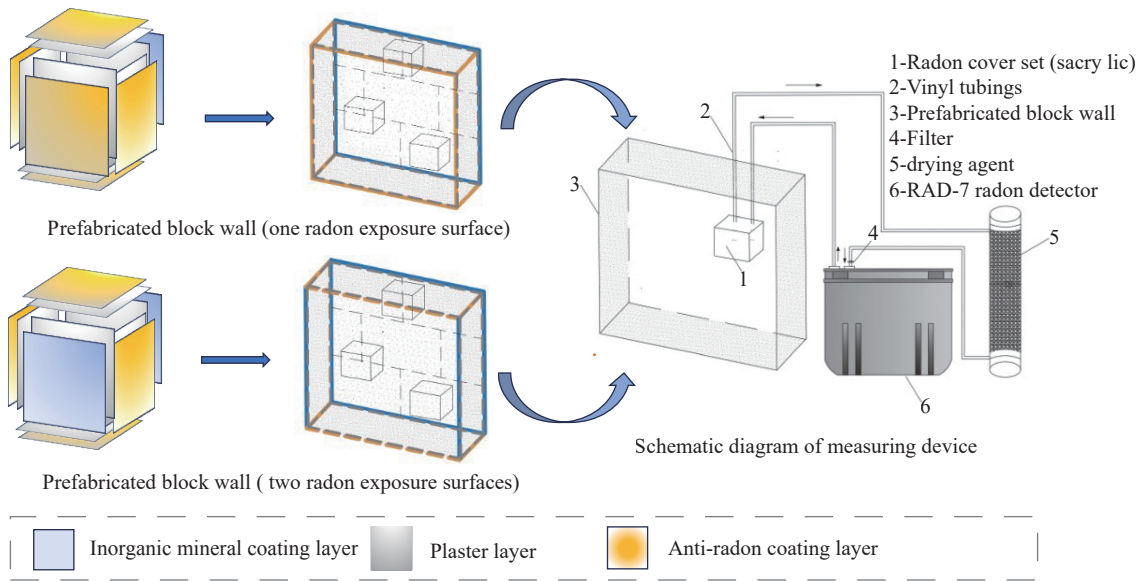


FIGURE 1. Schematic diagram of prefabricated block wall and experimental setup.

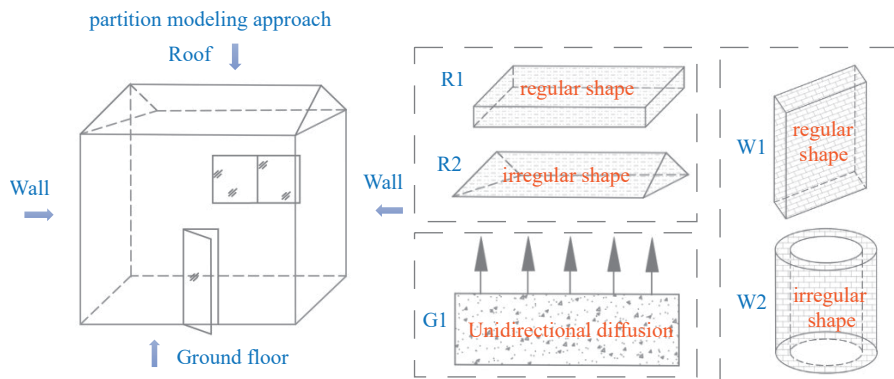


FIGURE 2. A schematic diagram illustrating the overall spatial structure of an indoor environment, including the shapes of different main building envelopes.

Notes: R1 is the roof of regular shape; R2 is the roof of irregular shape; W1 is the wall of regular shape; W2 is the wall of irregular shape; G1 is the ground floor.

from each building envelope at varying temperatures and thicknesses under conditions where building materials are the primary radon source and windows and doors remain closed. For scenarios where the bottom layer consists of soil and outdoor radon primarily originates from soil exhalation, we derived an expression for indoor radon concentration under ventilated conditions with open windows.

## RESULTS

### Measurement of Radon Activity Concentration and Surface Radon Exhalation Rate Fitting Function

Using autoclaved concrete blocks as raw materials,

we measured the surface radon exhalation rates of prefabricated block walls (one radon exposure surface) at three distinct thicknesses and five constant temperatures. Based on these measurements, we developed a fitting function to characterize the relationship between radon exhalation rate and the variables of temperature and wall thickness. The resulting fitting model is illustrated in Figure 3, with the corresponding mathematical expression presented in Equation (1).

$$H(X_{si}, T_{sj}) = -78.49982 + 804.1884X_{si} - 0.091T_{sj} - 1703.19947X_{si}^2 + 1.05192X_{si} \cdot T_{sj} \quad (1)$$

$T_{sj}(R^2 = 0.93376)$

In Equation (1),  $H(X_{si}, T_{sj})$  represents the surface radon exhalation rate of the building envelope within

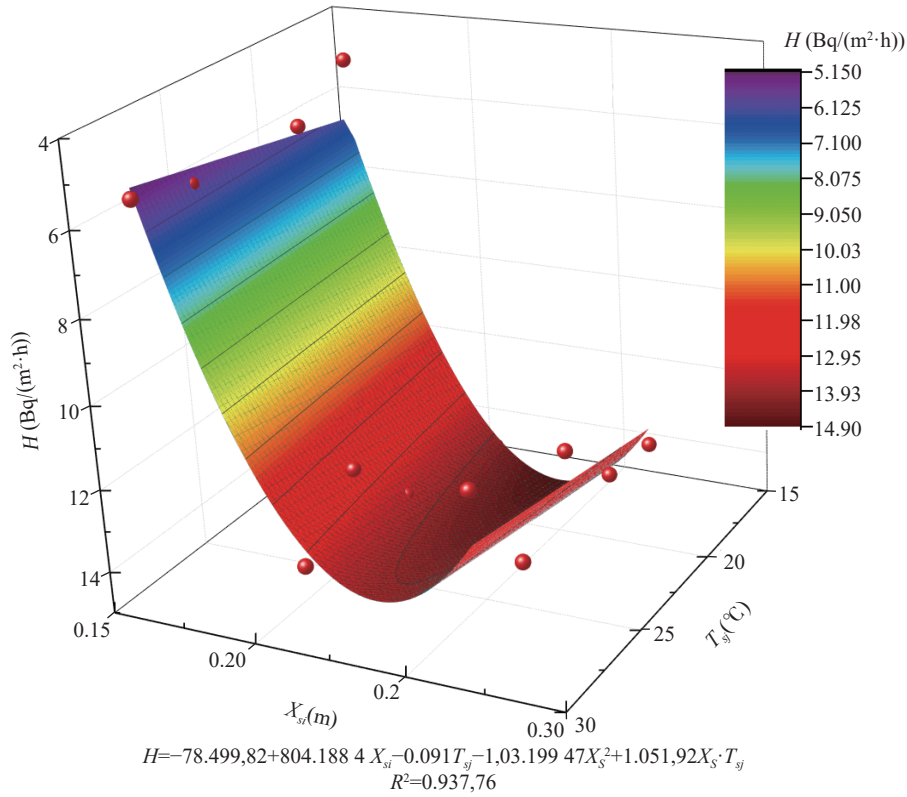


FIGURE 3. The fitting model of surface radon exhalation rate of block walls with varying temperatures and thicknesses. Notes:  $H$  is the radon exhalation;  $X_{si}$  is the structural thickness;  $T_{sj}$  is the indoor temperature;  $R^2$  is the goodness of fit.

the target room ( $\text{Bq}/(\text{m}^2 \cdot \text{h})$ );  $X_{si}$  denotes the thickness of the building envelope (m); and  $T_{sj}$  indicates the indoor temperature ( $^{\circ}\text{C}$ ).

### Expression for the Surface Radon Exhalation Rate from Walls with Multiple Materials

The total radon exhalation rate in walls composed of multiple materials can be expressed as the superposition of individual radon exhalation rates from each constituent material.

$$H(X_{si}, T_{sj}) = \frac{\sum_{k=1}^{k=z} H(X_{si}, T_{sj}) S_{sk}}{S} \quad (2)$$

In Equation (2),  $S_{sk}$  represents the actual exposed surface area ( $\text{m}^2$ ) of a specific material within the building envelopes;  $z$  represents kinds of materials;  $S$  denotes the total surface area of all building envelopes.

Surface area calculations vary by the type of building envelopes. For regular rectangular walls, as follows:

$$S_{sk1} = \theta_b \times \theta_w \quad (3)$$

Where,  $S_{sk1}$  is the actual exposed surface area of regular rectangular wall ( $\text{m}^2$ );  $\theta_b$  represents the height of wall (m);  $\theta_w$  represents the width of wall (m).

For building envelopes with curved interior surfaces, surface area calculations utilize geometric transformation relations, such as irregular arc walls, the structure is transformed into a cylindrical cavity, as follows:

$$S_{sk2} = \varepsilon_c h_c \quad (4)$$

Where,  $\varepsilon_c = 2\pi r_c$ ,  $S_{sk2}$  is the actual exposed surface area of irregular arc wall ( $\text{m}^2$ );  $\varepsilon_c$  represents the length of each curve (m);  $h_c$  represents the height of wall (m).

### Expression of A Prediction Model for Indoor Radon Concentration

For rooms where indoor radon primarily originates from construction materials, the radon concentration under natural air exchange conditions can be expressed by the following equation:

$$C(t) = \frac{H(X_{si}, T_{sj})S + \eta V_{eff} C_0}{\lambda_{eff} V_{eff}} + \left( \frac{H(X_{si}, T_{sj})S + \eta V_{eff} C_0}{\lambda_{eff} V_{eff}} - C_0 \right) e^{-(\lambda + R + \eta)t} \quad (5)$$

In Equation (5),  $C(t)$  represents the radon concentration ( $\text{Bq}/\text{m}^3$ );  $\lambda_{eff}$  is the effective decay constant (1/s);  $\lambda_{eff} = \lambda_{Rn} + R + \eta$ , 1/s;  $\lambda_{Rn}$  denotes the

radon decay constant,  $\lambda_{Rn} = 0.00756/h$ ;  $R$  represents the inverse diffusion coefficient, which characterizes the diffusion of indoor air radon into construction materials (1/s);  $\eta$  is the ventilation rate (1/h); and  $V_{eff}$  represents the effective room volume, defined as the total room volume minus the volume occupied by objects ( $m^3$ );  $C_0$  is the background radon concentration ( $Bq/m^3$ ).

When sufficient time has elapsed for indoor radon accumulation to reach equilibrium, the concentration can be calculated using:

$$C_{equ} = \frac{H(X_{si}, T_{sj})S + \eta V_{eff} C_0}{\lambda_{eff} V_{eff}} \quad (6)$$

In Equation (6),  $C_{equ}$  represents the concentration when indoor radon accumulation to reach equilibrium ( $Bq/m^3$ ). In typical residential buildings, the indoor ventilation rate exceeds the radon decay rate by more than two orders of magnitude. Therefore, both the radon decay and indoor anti-diffusion effects can be neglected, yielding  $\lambda_{eff} = \lambda_{Rn} + R + \eta \approx \eta$ . Under these conditions, Equation (6) simplifies to:

$$C_{equ} = \frac{H(X_{si}, T_{sj})S}{\eta V_{eff}} + C_0 = C_{H(X_{si}, T_{sj})} + C_0 \quad (7)$$

In Equation (7),  $C_{H(X_{si}, T_{sj})}$  is defined as the indoor radon concentration contributed by construction materials, which can be calculated using:

$$C_{H(X_{si}, T_{sj})} = \frac{H(X_{si}, T_{sj})S}{\eta V_{eff}} = \frac{\sum_{k=1}^{k=z} H(X_{si}, T_{sj})S_{sk}}{\eta V_{eff}} \quad (8)$$

The comprehensive expression for indoor radon concentration is:

$$C = \frac{\sum_{k=1}^{k=z} H(X_{si}, T_{sj})S_{sk}}{\eta V_{eff}} + C_0 \quad (9)$$

In Equation (9),  $C$  is defined as the indoor radon concentration ( $Bq/m^3$ ). For scenarios where the bottom layer consists of soil, the indoor radon concentration can be expressed as:

$$\phi(t) = \frac{\sum_{k=1}^{k=z} H(X_{si}, T_{sj})S_{sk} + \eta V_{eff} C_d}{\lambda_{eff} \lambda_{eff}} + \left( C_0 - \frac{\sum_{k=1}^{k=z} H(X_{si}, T_{sj})S_{sk} + \eta V_{eff} C_d}{\lambda_{eff} \lambda_{eff}} \right) e^{-\lambda_{eff} t} \quad (10)$$

In Equation (10),  $\phi(t)$  represents the total indoor radon concentration with a soil bottom layer in  $t$  time ( $Bq/m^3$ ), while  $C_d$  denotes the outdoor radon concentration generated by the soil layer ( $Bq/m^3$ );  $t$  represents time (h).

Given that  $\lambda_{eff} = \lambda_{Rn} + R + \eta \approx \eta$  and  $e^{-(\lambda+R+\eta)t} \approx 0$ , Equation (10) can be simplified to:

$$\phi = \frac{\sum_{k=1}^{k=z} H(X_{si}, T_{sj})S_{sk}}{\eta V_{eff}} + C_d \quad (11)$$

In Equation (11),  $\phi$  represents the total indoor radon concentration with a soil bottom layer ( $Bq/m^3$ ).

## The Application of the Prediction Model for Indoor Radon Concentration

We applied the prediction model for indoor radon concentration from construction materials to a radon simulation chamber (container house). Five prefabricated block walls of varying thicknesses (0.155 m, 0.165 m, 0.172 m, 0.213 m, and 0.268 m) as the sole radon sources within the chamber. The interior dimensions of the chamber measured  $2.80 \times 5.80 \times 2.50 m^3$ , featuring one door ( $0.90 \times 1.9 m^2$ ) and two windows ( $0.86 \times 0.93 m^2$ ). The effective volume of the chamber was  $38.78 m^3$ , representing 96% of the total interior volume. Temperature control was maintained using an air conditioning system.

During the winter experiment, doors and windows remained closed, resulting in low ventilation rates (5–7), which were approximated at 0.10–0.12 /h.

We calculated the indoor radon concentration under different ventilation rates at 23 °C and compared these values with the measured equilibrium radon concentration at the same temperature. The background radon concentration was  $6.50 Bq/m^3$ . The results are presented in Table 2.

## DISCUSSION

Indoor radon primarily originates from soil and building materials (8). Two critical factors influence indoor radon accumulation: surface radon exhalation rate and ventilation rate (9–11). We have established a prediction model for indoor radon concentration that incorporates the internal surface area and radon exhalation rate of the building envelope, indoor temperature, and natural air exchange rate, enabling accurate calculation of indoor radon concentration

TABLE 1. Comparison of calculated and measured radon concentration when equilibrium.

Ventilation rate (1/h)	Theoretical value (Bq/m <sup>3</sup> )	Measured value (Bq/m <sup>3</sup> )	Deviation (%)
0.10	21.25		7.76
0.11	19.91	19.60	1.56
0.12	18.80		4.26
0.13	17.85		9.80

under the combined influence of multiple factors.

A key strength of this model lies in its integration of building structural geometric parameters and environmental factors affecting indoor radon concentration. We developed a correlational function that accounts for radon exhalation rates across multiple walls at varying temperatures and thicknesses. The relationship between construction materials and indoor radon concentration has been optimized through direct measurement of surface radon exhalation rates from prefabricated walls, significantly enhancing the accuracy and broader applicability of indoor radon concentration predictions. For building envelopes with curved interior surfaces, we employed geometric transformation relationships to calculate wall surface areas. Through comparative analysis and validation, we demonstrated that the model's estimated indoor radon concentration from walls with thicknesses of 0.155–0.268 m at 23 °C aligns with measured values, with deviations less than 10%.

This refined model provides valuable guidance for preliminary building site selection, optimal door and window dimensioning, and scientifically informed selection of construction materials with respect to radon safety considerations.

While the model has limitations regarding daily and seasonal wall temperature fluctuations, as the fitting curve for exhalation rate calculations was derived from constant-temperature experiments, these constraints can be addressed by incorporating multiple fitting curves for various temperatures and wall thicknesses. Although there exists a discrepancy between modeled and real-world conditions, this deviation remains theoretically insignificant. Thus, the model maintains its practical utility and scientific validity within a controllable range.

**Conflicts of interest:** No conflicts of interest.

**Ethical Statements:** This research involves no ethical concerns as it does not include human/animal subjects or sensitive data.

doi: [10.46234/ccdcw2025.061](https://doi.org/10.46234/ccdcw2025.061)

# Corresponding author: Kuke Ding, [dingkk@chinacdc.cn](mailto:dingkk@chinacdc.cn).

<sup>1</sup> National Institute for Radiological Protection, Chinese Center for Disease Control and Prevention, Beijing, China; <sup>2</sup> Office for Public

Health Management, Chinese Center for Disease Control and Prevention, Beijing, China; <sup>3</sup> Key Laboratory of Beam Technology of Ministry of Education, School of Physics and Astronomy, Beijing Normal University, Beijing, China; <sup>4</sup> Institute for Radiation Hygiene Protection, Beijing Center for Disease Prevention and Control, Beijing, China.

Copyright © 2025 by Chinese Center for Disease Control and Prevention. All content is distributed under a Creative Commons Attribution Non Commercial License 4.0 (CC BY-NC).

Submitted: February 23, 2024

Accepted: February 24, 2025

Issued: March 14, 2025

## REFERENCES

1. Ting DSK. WHO handbook on indoor radon: a public health perspective. *Int J Environ Stud* 2010;67(1):100 – 2. <https://doi.org/10.1080/00207230903556771>.
2. Abbasi A, Mirekhtiary F, El-Denglawey A, Zakaly HMH. Influences of COVID-19 pandemic lockdown on excess lifetime cancer risk value of natural radiation. *J Radioanal Nucl Chem* 2021;329(3):1399 – 406. <https://doi.org/10.1007/s10967-021-07910-w>.
3. Ruano-Ravina A, Lema LV, Talavera MG, Gómez MG, Muñoz SG, Santiago-Pérez MI, et al. Lung cancer mortality attributable to residential radon exposure in Spain and its regions. *Environ Res* 2021;199:111372. <https://doi.org/10.1016/j.envres.2021.111372>.
4. Gooding TD. An analysis of radon levels in the basements of UK workplaces and review of when employers should test. *J Radiol Prot* 2018;38(1):247 – 61. <https://doi.org/10.1088/1361-6498/aaa18c>.
5. Chen YH, Chen YL, Wang QX, Li ZX, Chen P. Investigation and research on ventilation of naturally ventilated residences in China. *Heat Vent Air Cond* 2020;50(12):85 – 8,19. <https://doi.org/10.19991/j.hvac1971.2020.12.021>.
6. Hong YF, Dai ZZ, Chen X, Shen SL. Estimation of air exchange frequency in the condition of natural indoor ventilation. *J Environ Health* 2005;22(1):47 – 9. <https://doi.org/10.3969/j.issn.1001-5914.2005.01.018>.
7. Tan YL. Research on threshold value of average radon exhalation rate from indoor surface. *J Hengyang Norm Univ* 2016;37(3):30 – 3. <https://doi.org/10.13914/j.cnki.cn43-1453/z.2016.03.008>.
8. Mancini S, Guida M, Cuomo A, Guida D, Ismail AH. Modelling of indoor radon activity concentration dynamics and its validation through in-situ measurements on regional scale. *AIP Conf Proc* 2018;1982(1):020043. <https://doi.org/10.1063/1.5045449>.
9. Yarmoshenko I, Malinovsky G, Vasilyev A, Onishchenko A. Model of radon entry and accumulation in multi-flat energy-efficient buildings. *J Environ Chem Eng* 2021;9(4):105444. <https://doi.org/10.1016/j.jece.2021.105444>.
10. Sahoo BK, Nathwani D, Eappen KP, Ramachandran TV, Gaware JJ, Mayya YS. Estimation of radon emanation factor in Indian building materials. *Radiat Meas* 2007;42(8):1422 – 5. <https://doi.org/10.1016/j.radmeas.2007.04.002>.
11. Shahrokhi A, Kovacs T. Radiological survey on radon entry path in an underground mine and implementation of an optimized mitigation system. *Environ Sci Eur* 2021;33(1):66. <https://doi.org/10.1186/s12302-021-00507-w>.